# Endothelial Indoleamine-2,3-Dioxygenase-1 is not Critically Involved in Regulating Antitumor Immunity in the Central Nervous System

AP Abu Hejleh[1,2], K Huck[1,2], K Jähne[1,2], CL Tan[2], TV Lanz[1,3],
L Epping[4], JK Sonner[5], SG Meuth[4,6], A Henneberg[7,8], CA Opitz[7],
C Herold-Mende[9], F Sahm[10,11], M Platten[1,2] and K Sahm[1,2]

[1]Department of Neurology, Mannheim Medical Center, University of Heidelberg, Germany.
[2]DKTK Clinical Cooperation Unit Neuroimmunology and Brain Tumor Immunology, German Cancer Research Center, Heidelberg, Germany. [3]Department of Medicine, Division of Immunology and Rheumatology, Stanford University, CA, USA. [4]Department of Neurology with Institute of Translational Neurology, University Hospital Münster, Germany. [5]Institute of Neuroimmunology and Multiple Sclerosis, Center for Molecular Neurobiology Hamburg, University Medical Center Hamburg-Eppendorf, Germany. [6]Department of Neurology, Heinrich Heine University Düsseldorf, Germany. [7]Division of Metabolic Crosstalk in Cancer, German Consortium of Translational Cancer Research (DKTK) & German Cancer Research Center (DKFZ), Heidelberg, Germany. [8]Faculty of Bioscience, Heidelberg University, Germany. [9]Division of Neurosurgical Research, Department of Neurosurgery, University Hospital Heidelberg, Germany. [10]Department of Neuropathology, Heidelberg University Hospital, Germany. [11]DKTK Clinical Cooperation Unit Neuropathology, German Cancer Research Center (DKFZ), Heidelberg, Germany.

**ABSTRACT:** The vascular niche of malignant gliomas is a key compartment that shapes the immunosuppressive brain tumor microenvironment (TME). The blood-brain-barrier (BBB) consisting of specialized endothelial cells (ECs) and perivascular cells forms a tight anatomical and functional barrier critically controlling transmigration and effector function of immune cells. During neuroinflammation and tumor progression, the metabolism of the essential amino acid tryptophan (Trp) to metabolites such as kynurenine has long been identified as an important metabolic pathway suppressing immune responses. Previous studies have demonstrated that indoleamine-2,3-dioxygenase-1 (IDO1), a key rate-limiting enzyme in tryptophan catabolism, is expressed within the TME of high-grade gliomas. Here, we investigate the role of endothelial IDO1 (eIDO1) expression for brain tumor immunity. Single-cell RNA sequencing data revealed that in human glioma tissue, IDO1 is predominantly expressed by activated ECs showing a JAK/STAT signaling pathway-related CXCL11$^+$ gene expression signature. In a syngeneic experimental glioma model, eIDO1 is induced by low-dose tumor irradiation. However, cell type-specific ablation of eIDO1 in experimental gliomas did not alter frequency and phenotype of tumor-infiltrating T cells nor tumor growth. Taken together these data argue against a dominant role of eIDO1 for brain tumor immunity.

**KEYWORDS:** Indoleamine-2,3-dioxygenase-1 (IDO1), tumor vasculature, glioma, CNS immunity

## Introduction

Malignant gliomas are characterized by an immunosuppressive TME that not only consists of various pro-tumorigenic immune cell subsets such as tumor-associated macrophages or regulatory T cells but also comprises the vascular niche.[1] It is widely known that the brain tumor vasculature plays an essential role in regulating T cell transmigration and activity through the BBB.[2,3] This is of particular importance for brain tumor immunotherapy: Here, one major obstacle is to ensure homing of peripherally activated adaptive immune cells to the tumor while retaining their effector function. One immunosuppressive pathway restricting anti-tumor immunity is mediated by the catabolism of the essential amino acid Trp to immunosuppressive downstream metabolites.[4,5] IDO1 is the first and rate-limiting

enzyme of the tryptophan catabolism and serves as an immune checkpoint.[6] Both Trp depletion and kynurenine (Kyn) accumulation contribute to local immunosuppression by suppressing proinflammatory T cell responses and promoting the activation of regulatory T cells and myeloid-derived suppressor cells, respectively.[7-9] In addition, IDO1 facilitates tumor formation by promoting neovascularization characterized by extensive and dysfunctional blood vessels.[10,11] Hence, its expression correlates with the malignancy of gliomas.[12-14] Several studies have shown that tumoral IDO1 expression induce the accumulation of immunosuppressive regulatory T cells and suppress T cell migration and function by depletion of Trp. Within the immune compartment, IDO1 expression is not only confined to myeloid cells, which represent the largest population of IDO1$^+$ immune

cells, but induced by transmigrated effector T cells in an IFNγ-dependent manner.[14,15] Low-dose irradiation increases the response to immunotherapy by reshaping the TME.[16] Blocking eIDO1 could help to boost the beneficial effect of low-dose irradiation in triggering an effective anti-tumor T cell response. We have previously shown that IDO1 is strongly expressed in glioma-associated endothelial cells.[5] However, while the role of tumor- and innate immune cell-derived IDO1 has been extensively studied, its angiocrine role on tumor-specific T cell recruitment and effector function in glioma and the implication for brain tumor immunotherapy remains ambiguous. In this study, we exploit the functional relevance of eIDO1 expression for recruitment and effector function of tumor-specific T cells in human gliomas and a syngeneic murine glioma model.

## Materials and Methods

### Cell culture

GL261 and GL261-gp100 cells were cultured in Dulbecco's modified Eagle's medium (DMEM) supplemented with 10% fetal bovine serum (FBS), 100 U/ml penicillin, and 100 μg/ml streptomycin (Sigma-Aldrich) at 37°C, 5% $CO_2$.[17] Primary murine CD31+ EC were isolated from cerebral hemispheres of C57BL/6J wildtype (WT) mice by using the Miltenyi MACS endothelial cell isolation kit and were cultured in EBM-2 basal medium with supplements (Lonza, EGM™-2-MV BulletKit™, CC-3202) at 37°C, 5% $CO_2$ according to the manufacturer's instructions.

### High-performance liquid chromatography

For high-performance liquid chromatography (HPLC), cells were stimulated with 10 μg/ml IFNγ for 24 hours and cell culture supernatant was analyzed for kynurenine and tryptophan quantities. Protein precipitation was based on 33.73 μl 72% trichloroacetic acid to a defined volume of 200 μl supernatant followed by centrifugation at maximum speed for 10 minutes. Subsequently, supernatants were transferred into glass HPLC vials and were further analyzed for respective enzyme levels.

### Mice

Six- to nine-week-old male and female mice were maintained in a special pathogen-free, temperature-controlled (22 ± 1°C) mouse facility on a reverse 12-hour light, 12-hour dark cycle at the DKFZ, Heidelberg. C57BL/6J WT mice were purchased from The Jackson Laboratory and floxIDO X VE-Cadherin-Cre mice were generated and bred at the animal facility of the DKFZ, Heidelberg. Pmel-1/luc-mcherry mice were generated by crossing pmel-1 mice with luc-mcherry mice. Luc-mCherry mice express luciferase and mCherry under the Actb promotor and were generated in the Transgenic Service of the Center for Preclinical Research, DKFZ, Heidelberg. All animal experiments were performed according to the guidelines of the German Animal Welfare Act and approved by the governmental authorities (Regional Administrative Authority Karlsruhe, Germany).

### Generation of murine CD90.1+ CD8+ CTL

CD90.1+ CD8+ T cells were isolated from spleens and lymph nodes of 6 to 10 weeks old pmel-1 or pmel-luc-mcherry mice and excised and meshed through a 70 μm cell strainer. After lysis of erythrocytes with ACK lysis buffer (150 mM $NH_4Cl$, 10 mM $KHCO_3$, and 100 μM $Na_2EDTA$), the isolated immune cells were cultured in murine T cell proliferation medium consisting of RPMI-1640 (Sigma-Aldrich) supplemented with 10% FBS, 100 U/ml penicillin, 100 μg/ml streptomycin, 25 mM Hepes pH 7.4, 1 mM sodium pyruvate, $5 \times 10^{-5}$ M 2-mercaptoethanol (all Sigma-Aldrich) and 2 mM l-glutamine (Thermo-Fisher) under stimulation with 30 IU/ml IL-2 (Proleukin, Novartis) and 2 μg/ml $hgp100_{25-33}$ (custom-made; Research Group GMP & T cell thrapy, DKFZ) for 3 days at 37°C, 5% $CO_2$. For adoptive cell transfer, CD90.1+ CD8+ T cells were isolated by using mouse CD8+ T cell isolation MACS Kit (MACS Miltenyi Biotec) according to the manufacturer's instruction. CD90.1 is a surface protein particularly abundant on peripheral T cells enabling a clear distinction between donor and recipient tumor infiltrating immune cells.[18]

### Tumor challenge and treatment

A total of $1 \times 10^5$ GL261-gp100 tumor cells were diluted in 2 μl sterile phosphate-buffered saline (PBS; Sigma-Aldrich) and stereotactically implanted into the right hemisphere 2 mm right lateral of the bregma and 1 mm anterior to the coronal suture of 6- to 9-week-old floxIDO X VE-Cadherin-Cre mice and their littermate control mice with an injection depth of 3 mm below the dural surface. Tumor cell inoculation was performed under anesthesia using a 10 μl gas-tight Hamilton micro-syringe driven by a fine step stereotactic device (Stoelting). Mice received analgesics for 2 days post operation and were checked daily for tumor-related symptoms and sacrificed when tumor size reached 6 mm or mice showed signs of neurological deficit. To monitor tumor growth, MRI was performed on day 8 and 15 post inoculation. For radiotherapy, mice received 4 fractions à 2 Gy starting from day 9 or 10 as indicated. For adoptive T cell transfer (ACT), $5 \times 10^6$ pmel-1 CD90.1+ CD8+ T cells were intravenously injected at day 7 after inoculation followed by injection of 50 000 IU IL-2 intra-peritoneally for 2 subsequent days.

### In vivo bioluminescent imaging

To track adoptively transferred T cells, we used the In vivo imaging system (IVIS) Lumina Series III from Perkin Elmer at days 1 to 2 after ACT. Prior to imaging, mice were shaved at the body regions of interest, injected with 50 mg/kg d-Luciferin s.c.

(StayBrite™, BioVision, Mountain View) and anesthesia was induced with isoflurane 3% to 4%. Bioluminescence images (BLI) were acquired 10 minutes after D-Luciferin injection with an exposure time of 30, 45, and 60 seconds. During imaging, mice were kept under anesthesia with isoflurane 1.5%. Bioluminescent data were acquired and analyzed using Living Image 4.3 Software (Perkin Elmer). BLI quantification was performed by setting regions of interest (ROI) around the tumor area and signals were quantified as photons/second. For each experiment, ROIs were kept identical during all time points.

## Processing of spleen, blood, and tumor tissue

For the isolation of tumor infiltrating lymphocytes, mice were sacrificed by terminal cardiac perfusion and the tumor-bearing right hemisphere was excised and the cerebellum removed. Whole tumor tissue were mechanically dissected and enzymatically digested in HBSS (Sigma-Aldrich, 11088866001) supplemented with 50 µg/ml Liberase DL (Roche) under slow rotation at 37°C for 30 minutes. Digested tumors were meshed twice through a 100 µm and a 70 µm cell strainer to obtain single-cell suspension. Tumor cell suspensions were purified by removal of myelin with 4.5 ml Percoll (Sigma/GE, 17-0891-01). Blood samples were obtained by cardiac puncture and collected in syringes coated with 0.5 M EDTA. Spleens were excised and meshed twice through a 70 µm cell strainer, followed by lysis of erythrocytes in ammonium-chloride-potassium (ACK) Lysis Buffer (150 mM $NH_4Cl$, 10 mM $KHCO_3$, and 100 µM $Na_2EDTA$). Tumor draining lymph nodes were excised from the cervical and axillary region of the mouse. For further processing, lymph nodes were meshed through a 70 µm cell strainer to obtain a single-cell suspension.

## Histology

Formalin-fixed, paraffin-embedded WHO grade 3 to 4 primary and recurrent human glioma tissues were obtained from the archives of the Department of Neuropathology, Heidelberg and were cut to 3 µm sections and processed using a Ventana Benchmark Ultra immunostainer. The DAB staining procedure included blocking of endogenous peroxidase with 0.3% $H_2O_2$ for 3 minutes and treatment with blocking buffer, followed by incubation with the primary antibody at 4°C overnight. Incubation was followed by ABC-Kit-Solution for 30 minutes, washing and counter-staining with hematoxylin for 2 minutes. Positivity was visualized with 3′3 diaminobenzidine (DAB; brown) using the ultraView Universal DAB Detection Kit (Ventana Medical Systems, Inc.). The following primary antibodies were used: anti-human CD8 (1:50, Dako M7103), anti-human CD3 (1:200, Thermo Scientific #RM-9107-S), anti-human CD31 (1:10, Dako M0823), and anti-human IDO1 (1:200, Cell Signaling Technology). Density of IDO1$^+$ cells was evaluated semiquantitatively by overall impression at low microscopic magnification (100×)

within 1 mm² and if any specific positive staining was identified it was judged present.

## RNAScope®

For novel in situ hybridization using Advanced Cell Diagnostics RNAScope® probes and reagents, mice were sacrificed by cardiac perfusion with PBS and excised brains were treated with 4% PFA for 4 hours followed by a transfer into 30% sucrose solution at 4°C for 24 to 48 hours. Subsequently, isolated brains were then embedded in Tissue-Tek O.C.T.Tm (Sakura) and slowly frozen down on liquid nitrogen. Fresh frozen samples were cut to 10 µm sections and treated with the Fluorescent Multiplex protocol according to the manufacturer's instruction. Briefly, tissue sections were permeabilized with 1X Target retrieval solution followed by a treatment with 5 drops of protease IV at RT for antigen accessibility. The following probes were then hybridized for 2 hours at 40°C in a HybEZ™ II Oven: IDO1 (cat. No. 323104-C1), Cdh5 (cat. no. 323105-C2) to reveal the expression of IDO1 in ECs. Subsequently, amplifier probes were added, and signal visualization was performed through probe-specific HRP-based detection by Opal dyes. Slides were then incubated for 30 seconds with DAPI and coverslipped with ProLong Gold Antifade Mountant medium. Images were acquired using a Zeiss LSM 710 ConfoCor 3 microscope with 20× magnification and analyzed in ImageJ software (v1.50i, NIH, Bethesda, USA).

## Flow cytometry analysis

Single cell suspensions were stained with the following fluorescent antibodies against surface antigens: BV510-conjugated anti-mouse CD45 (BioLegend; 30-F11; 103138), APC-Cy7-conjugated anti-mouse CD3 (BioLegend; 17A2; 100222), PerCP Cy5.5-conjugated anti-mouse CD25 (BioLegend; PC61; 102030), AF700-conjugated anti-mouse CD8 (BioLegend; 53-6.7; 100730), BV605-conjugated anti-mouse CD4 (BioLegend; RM4-5; 100548), BV421-conjugated anti-mouse PD-1 (BioLegend; 29F.1A12; 135218), PE-conjugated anti-mouse CD90.1 (BioLegend; OX-7; 202524). For intracellular antigen targets, cells were incubated with 20 µg/ml gp100 and 10 µg/ml Brefeldin A in T cell medium for 4 hours at 37°C. Next, a FoxP3/transcription factor staining buffer set (eBioscience; 00-5523) was applied and following fluorescently labeled antibodies against intracellular molecules were used: PE-Cy7-conjugated anti-mouse IFNγ (Thermo Fisher; XMG1.2; 4332567), BV605-conjugated anti-mouse Ki67 (BioLegend; 16A8; 652413), APC-conjugated anti-mouse FoxP3 (Invitrogen; FJK-16a; 2107506). Flow cytometry acquisition was performed on BD FACS LSR Fortessa (BD Biosciences, Heidelberg, Germany) using the BD FACSDiva software. FlowJo V10 was used for data analysis.

*Single cell analysis*

Single cell transcriptomic data of glioblastoma was obtained from UCSC Cell Browser (https://gbm.cells.ucsc.edu) and imported into R for further analysis. Cells were annotated as given by the metadata. Endothelial cells were subsequently subset out and reanalyzed using Seurat. Subsetted data was first normalized using sctransform implemented in Seurat and then visualized using UMAP. Unsupervised clustering was done and key marker genes for each cluster were identified using FindAllMarkers function. For pathway analysis, PROGENy is used to estimate the up- and down-regulation of signaling pathway.

*Graphical representation and statistics*

All data are presented as means ($\pm$SEM, SD) as indicated in figure legend. Significance was either assessed by unpaired two-tailed t-test or Mann-Whitney test. $P < .05$ was considered statistically significant ($P < .05$, $P < .01$, $P < .001$). Statistics were calculated using GraphPad Prism 8.0.

## Results

### IDO1 is expressed in human glioma–associated endothelial cells and restricted to a CXCL11+ cell cluster

To analyze the expression pattern of IDO1 in the vascular compartment of human malignant gliomas WHO grade 3 and 4, a set of 13 paired primary and recurrent glioma specimens was analyzed by immunohistochemistry. Recurrent high-grade gliomas showed overall a slightly higher number of IDO1+ cells compared to primary tumors. While based on histomorphological criteria tumor cells themselves hardly showed any IDO1 staining which is in line with previously published data demonstrating low IDO1 expression levels in neoplastic and myeloid cells of human GBM tissue,[19,20] tumor blood vessels in recurrent high-grade gliomas expressed IDO1 (Figure 1A). To validate this result in an independent data set and to detect IDO1 expression in a cell type specific manner, we next investigated the expression profile of IDO1 in scRNA-seq data retrieved from the UCSC cell browser, analyzing 11 untreated primary GBM.[21,22] Here, IDO1 was mainly expressed in the endothelial compartment (Figure 1B) and unsupervised clustering of CD31+ endothelial cells revealed 4 distinct subsets with IDO1 expression being confined to a CXCL11-positive cluster (Figure 1C and Supplemental Figure S2), primarily characterized by activated JAK/STAT signaling and expression of IFNγ-like GBP1 and interferon-stimulated gene 15 (ISG15) (Figure 1D).[23,24] The remaining endothelial subclusters SLN, CD34, and NDRG1 expressed little to no IDO1. These findings suggest that similar proinflammatory cues induce CXCL11 and IDO1 and support the notion that tumor ECs exhibit extensive heterogeneity with respect to an inflammatory signature.[25,26] Of note, endothelial expression levels of TDO2, another enzyme catabolizing tryptophan to kynurenine in GBM, were low.

### eIDO1 expression and activity in mouse brain microvascular endothelial cells

To confirm that the tryptophan metabolism is active in murine EC we isolated brain microvascular endothelial cells (MBMEC) from wildtype mice and eIDO cKO mice. Depletion of eIDO resulted in significantly lower kynurenine levels in the cell culture supernatant (Figure 2A). To investigate the functional role of eIDO1 in gliomas, we made use of a syngeneic orthotopic GL261 glioma model expressing the tumor-associated antigen gp100. IDO1 was expressed in endothelial cells in GL261-gp100 tumors shown by its co-localization with vascular endothelial cadherin (VE-cadherin) (Figure 2B). To assess the effect of endothelial IDO on the transmigration and effector function of tumor-specific T cells, we generated eIDO1-specific conditional knockout mice (eIDO cKO), where eIDO1 was conditionally ablated in ECs expressing VE-cadherin (Figure 2C).[27]

### Ablation of eIDO1 does not impact response of experimental glioma to low–dose radiotherapy

Irradiation of human brain ECs resulted in the upregulation of IDO1 (Supplemental Figure S1). A previous study has shown that radiotherapy synergizes with pharmacological inhibition of IDO1 to increase tumor-infiltrating cytotoxic T cells.[28] To further investigate the effect of eIDO1 deficiency on radiation-induced immune cell infiltration we performed an intracranial tumor injection followed by 4 times low-dose radiotherapy. To confirm tumor growth, we implemented MRI imaging on day 8 and 15 (Figure 3A). While there is no significant effect on tumor size (Figure 3B), we did observe a slight but significant influx in CD4+ T cells and a slightly increased expression of programed cell death protein 1 (PD1) as exhaustion marker on CD8+ T cells in eIDO1 deficient mice (Figure 3C). Interestingly, loss of eIDO1 did neither affect Treg cells nor attract CD8+ T cells (Figure 3C). These data suggest that while eIDO1 deficiency does not augment total T cell infiltration or tumor control it is still associated with a slight shift of the immune cell infiltrates toward CD4+ T cells.

### Conditional eIDO1 knockout does not alter transmigration and effector function of antigen–specific CD8+ T cells

Recent findings of our group showed that low-dose radiotherapy of orthotopic gliomas in combination with adoptive T cell therapy resulted in a marked increase in the recruitment of activated CD8+ T cells. That is why we implemented an adoptive T cell transfer of antigen-specific CD8+ T cells to investigate
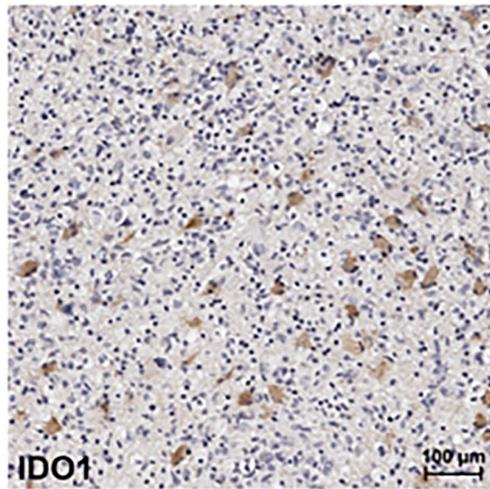
**A**
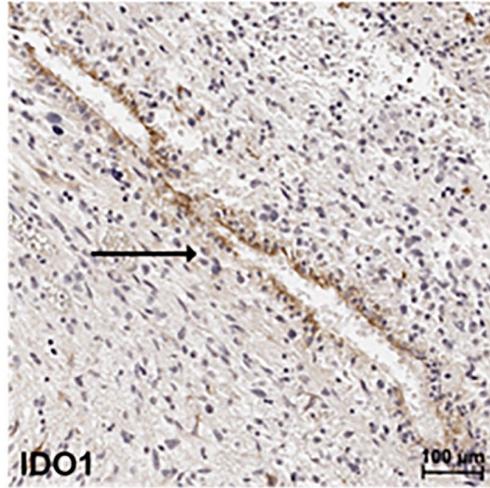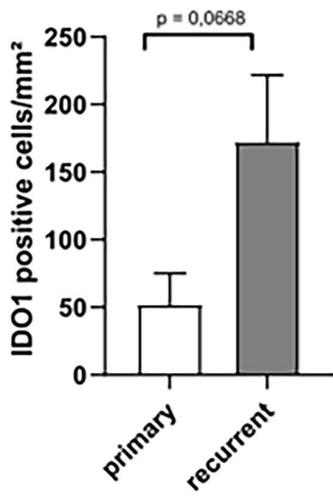


IDO1
recurrent GBM WHO grade IV
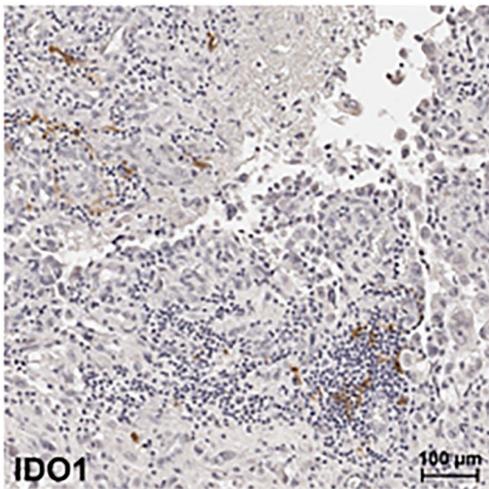


IDO1
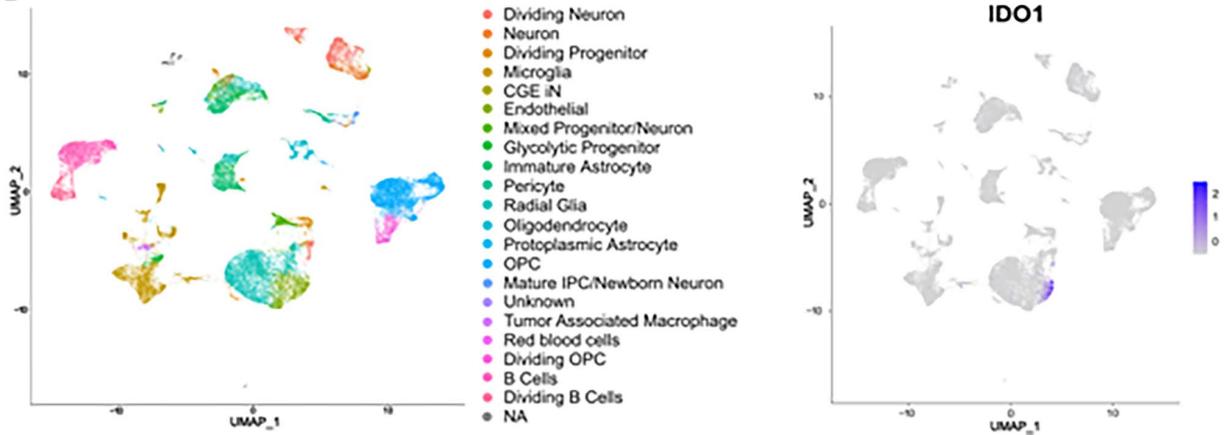primary GBM WHO grade IV



IDO1
recurrent GBM WHO grade IV

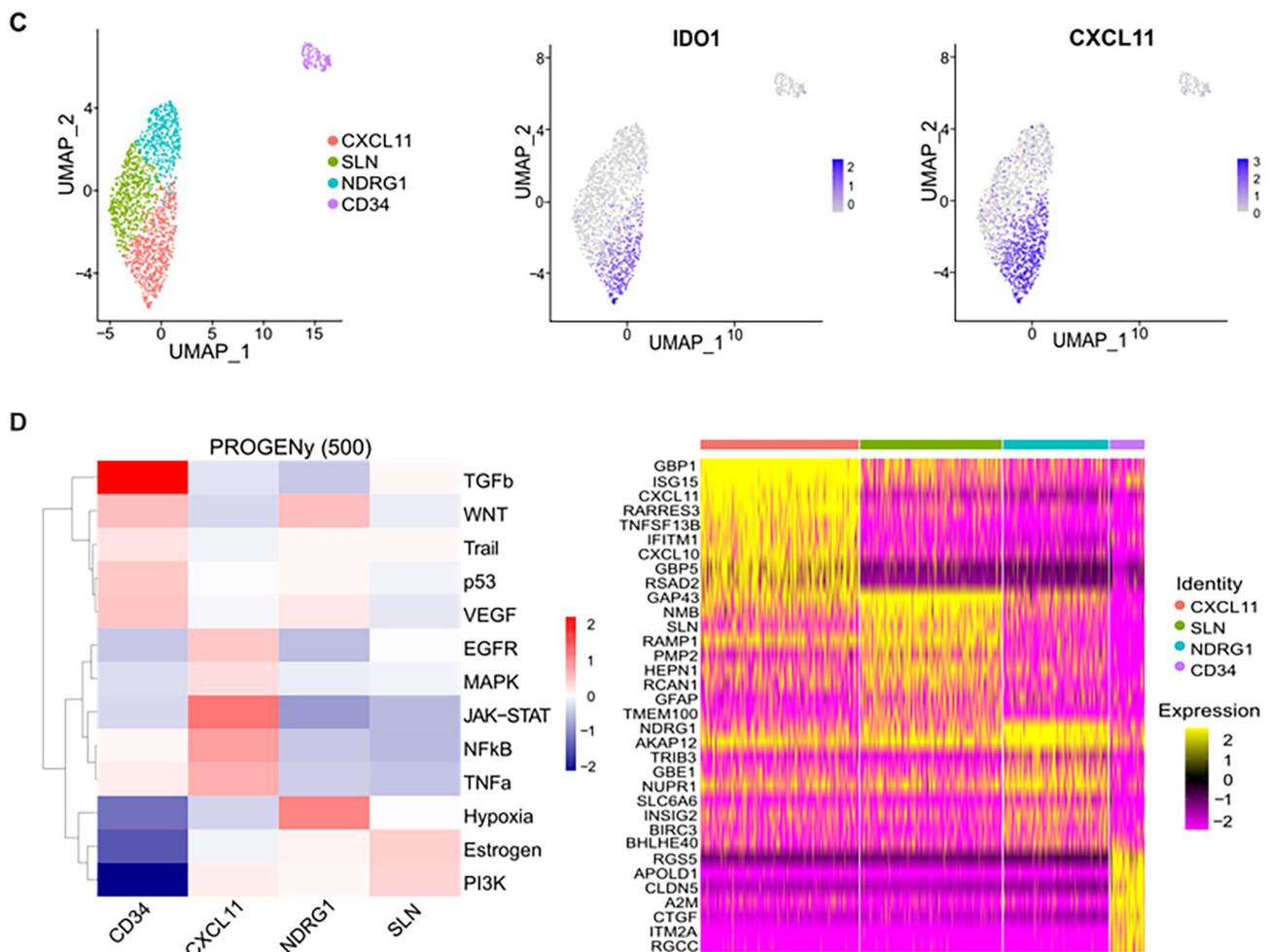**B**



**Figure 1.** *(Contiunued)*

**Figure 1.** IDO1 is expressed in human glioma-associated endothelial cells and confined to a CXCL11-positive endothelial cell cluster. (A) Quantitative analysis of IDO1+ cells in primary and recurrent WHO grade 3 and 4 human glioma within 1 mm² and representative IHC stainings of primary and recurrent human gliomas with IDO1 specific antibodies. Number of IDO1+ cells is slightly increased in recurrent human glioma. Arrow indicates IDO1 positive ECs in recurrent GBM WHO grade 4. Data is presented as mean SEM. For (A) statistical significance was defined by a paired student's t-test. (B) UMAP (Uniform Manifold Approximation and Projection) projection of the UCSC dataset, color-coded by cell populations of primary GBM. IDO1 is predominantly expressed in ECs. (C) UMAP plot depicting distinct endothelial clusters upon analysis. IDO1 expression is limited to CXCL11+ cluster. (D) Pathway analysis of single-cell cluster-defining genes and heat map of RNA expression of single-cell cluster-defining genes.

the impact of conditional eIDO KO together with low-dose radiotherapy on peripheral T cell infiltration into the tumor. Therefore, we applied ACT of gp100-specific CD8+ T cells isolated from pmel-1 mice in addition to low-dose radiotherapy (Figure 4A). Pmel-1 mice carry a T cell receptor specific for gp100, an endogenous tumor-associated antigen (TAA) frequently expressed in human glioma.[29] Prior to injection, isolated T cells of pmel-Luc_mCherry mice underwent magnetic-based cell separation followed by stimulation with gp100 and IL-2.[30] This tripartite regimen stimulates the proliferation of injected T cells and enhances T cell recognition efficacy.[31] Also in this regimen, eIDO1 expression did not alter tumor size (Figure 4B). Four days after ACT, multicolor flow cytometry was used to analyze the phenotype of tumor-infiltrating leukocytes (TILs). Here, total influx of T cell subsets did not show any difference dependent on eIDO1 expression

(Figure 4C). Finally, ablation of eIDO1 did not impact the influx of adoptively transferred CD90.1+ CD8+ T cells as shown by IVIS (Figure 4D) and flow cytometry (Figure 4E).

## Discussion

It is widely accepted that IDO1 plays an important role in glioma-associated immunomodulation.[32] Thus, several clinical trials tested the pharmacological inhibition of IDO1 along with checkpoint inhibition which did not show any clinical benefit, emphasizing the existing gap of knowledge regarding the full biological consequences of IDO1 activity in the TME.[33,34] While most studies have investigated the role of IDO1 and other tryptophan metabolizing enzymes like TDO expressed by glioma cells and various immune cell populations,[5,35] its function in the vascular compartment, specifically in ECs, and contribution to the immunosuppressive TME
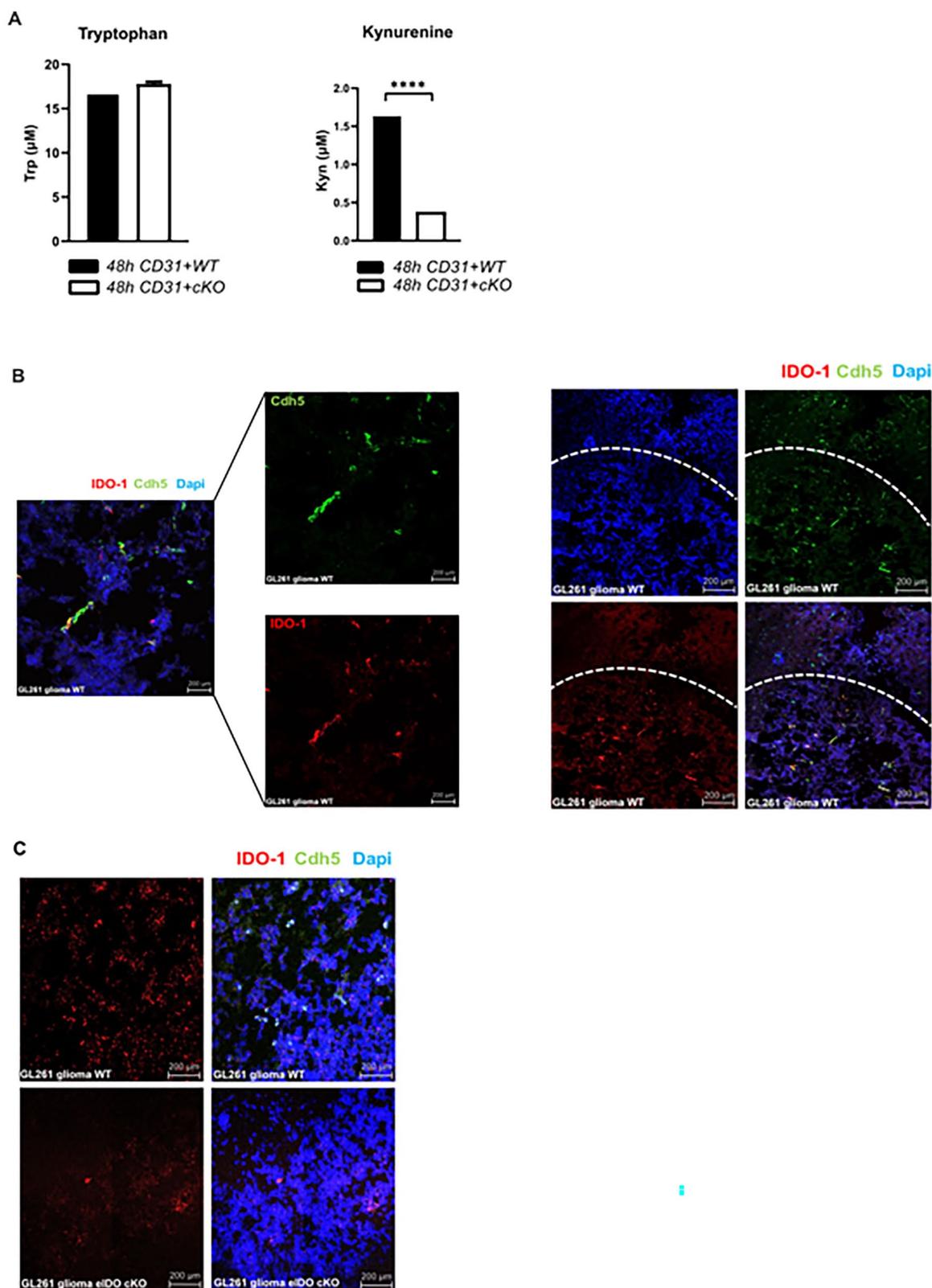
**Figure 2.** Kynurenine is downregulated in mouse brain microvascular endothelial cells (MBMEC) of eIDO cKO mice. ECs were purified from C57BL/6J WT mice and eIDO cKO mice by using the Miltenyi MACS endothelial cell isolation kit. Cell supernatants were harvested after 48 hours to quantify kynurenine and tryptophan via HPLC. (A) After 48 hours tryptophan concentration remained unchanged whereas kynurenine levels were significantly decreased in eIDO cKO mice. For (A), statistical significance was determined by a two-tailed student's t-test (****$P < .0001$). (B) Visualization of eIDO1 expression in GL261-gp100 glioma by RNAScope®. Coronal sections of murine GL261-gp100 glioma in WT mice were co-stained for *Ido1* and *Cdh5* mRNA, using RNAscope® Technology. IDO1 expression is mainly confined to GL261 glioma tissue. (C) Endothelial *Ido1* expression in coronal sections of GL261 glioma in WT and eIDO KO mice.
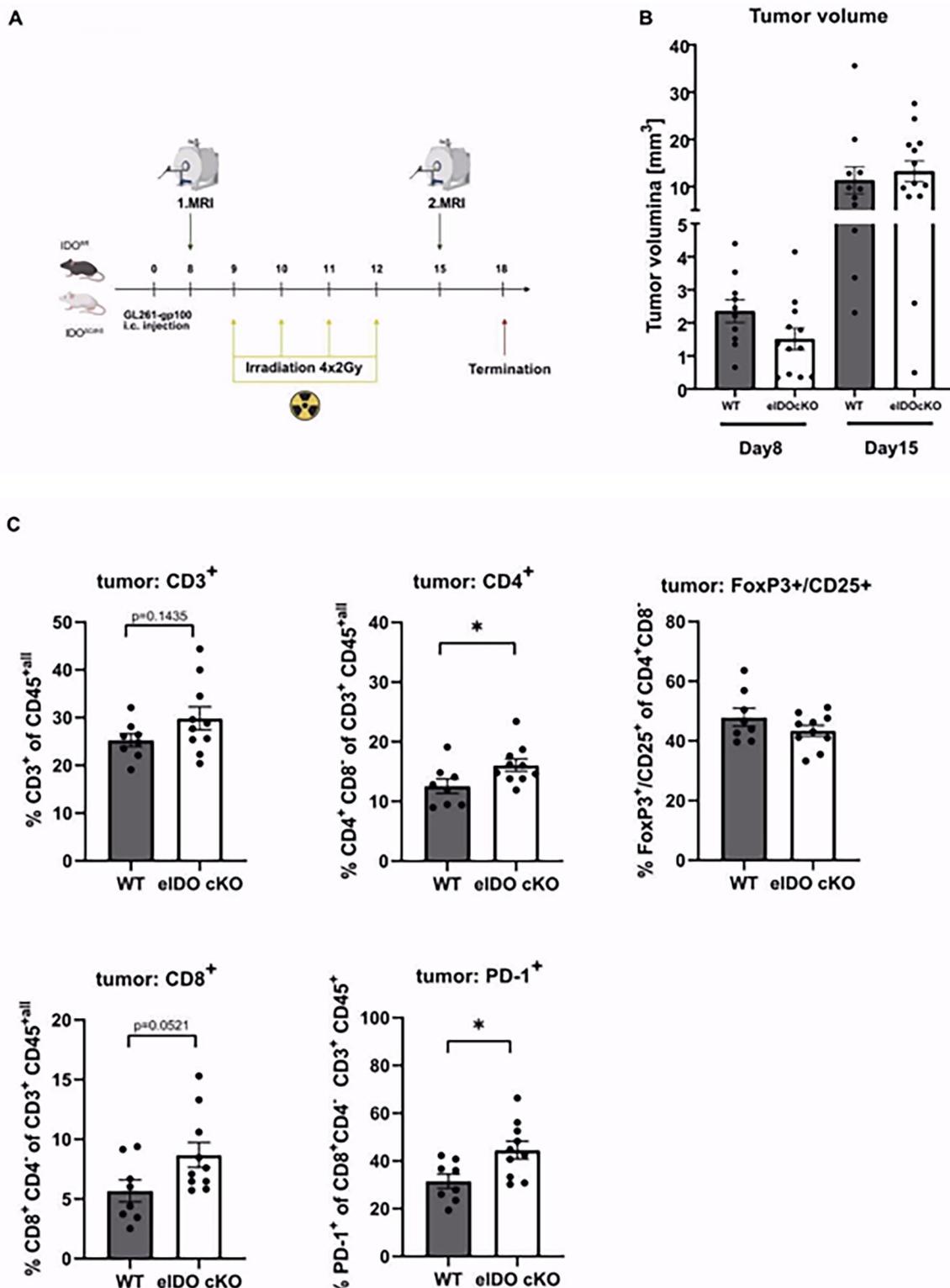
**Figure 3.** eIDO1 deficiency together with irradiation induced immune stimulation leads to shift toward CD4+ T cell infiltration. (A) GL261-gp100 cells were inoculated in floxIDO X VE-Cadherin-Cre mice (eIDO cKO) and littermate control mice (n = 11 vs n = 14 animals). Low-dose radiotherapy à 2 Gy was implemented for four subsequent days starting at day 9. (B) Tumor growth was measured with MRI on day 8 and 15. (C) TILs were isolated and analyzed with flow cytometry for T cell frequency and further subsets: CD4+ T cells, CD8+ T cells, PD1 expression on CD8+ T cells, and regulatory T cells. All data are presented as mean SEM. For (C) statistical significance was defined by a two-tailed student's t-test in combination with Mann-Whitney test (*$P < .05$, **$P < .01$, ***$P < .001$).
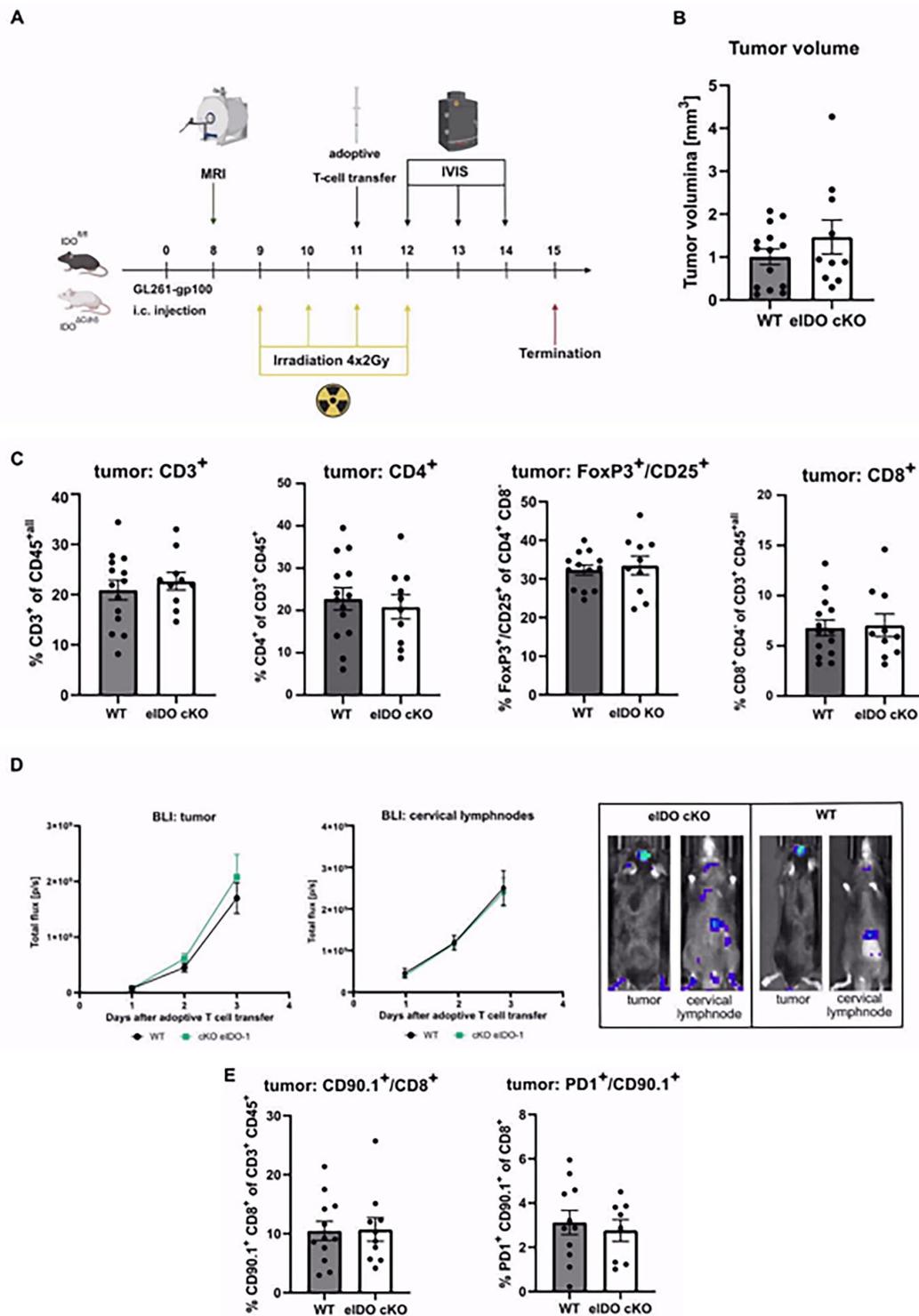
**Figure 4.** Conditional eIDO1 knockout does not alter transmigration efficacy and effector function of gp100-specific CD90.1⁺ CD8⁺ T cells. (A) GL261-gp100 cells were inoculated in floxIDO X VE-Cadherin-Cre mice and littermate control mice (n=14 vs n=10 animals). An adoptive T cell transfer with gp100-specific tumor-infiltrating cytotoxic T cells was performed at day 11 in addition to a low-dose radiotherapy. (B) Tumor volumes were measured with MRI on day 8. Immunophenotyping did not reveal any T cell-intrinsic differences as a result of eIDO1 knockout. (C) TILs were isolated and analyzed with flow cytometry for T cell frequency and differentiated into CD4⁺ T cells, CD8⁺ T cells, and regulatory T cells. (D) Tracking of adoptively transferred T cells was performed with in vivo bioluminescent imaging. Quantification of bioluminescence signals from luciferase expressing cytotoxic T cells in the tumor and the draining cervical lymph nodes measured from day 12 to day 14. In vivo bioluminescence imaging of infiltrating adoptively transferred T cells in tumor and draining cervical lymph nodes by IVIS Lumina Series III with an exposure time of 30, 45, and 60 seconds. (E) Flow cytometry analysis of CD90.1⁺ CD8⁺ T cells and CD90.1⁺ T cells with an exhaustion signature (PD1+).

remain elusive. In this study, we analyzed the expression of eIDO1 in human glioma samples and investigated the impact of eIDO1 deficiency, combined with T cell immunotherapy and low-dose radiotherapy, on controlling and shaping the local immunomodulatory T cell compartment with a particular focus on the immune-vascular interface in experimental gliomas.

To assess the role of eIDO1 in human glioma, we analyzed the expression of eIDO1 in primary and recurrent grade 3 and 4 human glioma by immunohistochemistry and detected eIDO1 only in recurrent high-grade glioma (Figure 1A). To date, the standard therapy of primary GBM consists of radiotherapy, surgery and temozolomide chemotherapy.[36] One possible explanation for the expression of eIDO1 in recurrent GBM could be the consequence of previous irradiation-induced immune stimulation that led to an upregulation of pro-inflammatory cytokine levels, inducing eIDO1 expression.

A novel aspect from our analysis of scRNA-seq data of human GBM found that tumor-associated ECs exhibit a well-defined heterogeneity that can be divided into 4 clusters (Figure 1C and D). Interestingly, eIDO1 is restricted to a subpopulation characterized by the expression of the interferon-induced protein CXCL11 (Figure 2C). CXCL11, also known as inducible T cell-α chemoattractant (I-TAC), is a chemokine unfolding its effect by binding to CXCR3 on target cells.[37,38] Previous studies identified CXCL11 in tumor-associated vasculature in human GBM and meningioma.[39,40] Notably, higher CXCL11 quantities were found in GBM specimen compared to low-grade gliomas or in normal brain tissue.[41] Expression of IDO1 and the respective chemokines is part of an IFNγ-related response and thus potentially intertwined.[42,43] With this finding, it is tempting to assume a mutual influence of the CXCL11-CXCR3 axis on eIDO1 activation and vice versa. Currently, we are lacking knowledge about comprehensive signaling pathways inducing IDO1 expression in ECs. Although eIDO cKO significantly influences kynurenine levels in our model, the role of eIDO1 may additionally be masked by the impact of IDO1 and TDO expressed by cancer cells and immune cell populations.[13] Several publicly available scRNA-seq data sets from a total of 7 patients with primary GBM revealed rather low expression of IDO1 in neoplastic cells and myeloid cells but a co-localization of CXCL11 and eIDO emphasizing the interindividual heterogeneity of IDO1 expression in human GBM.[19,20] However, one limitation of scRNA-seq is the lack of capturing all possible IDO1 isoforms, whereas Smartseq full-length sequencing is required to identify all potential isoforms.

To characterize its function in murine ECs we implemented conditional eIDO1 knockout mice in a syngeneic orthotopic GL261-gp100 model. Based on the finding that local irradiation synergizes with adoptive T cell transfer by enhancing the proliferation and effector function of transferred T cells and exposing tumor associated antigens,[44,45] we applied either low-dose radiotherapy or combined irradiation with an adoptive T cell transfer. In experimental GL261-gp100 gliomas, loss of eIDO1 was not sufficient to facilitate the recruitment of transmigrating T cells (Figures 3 and 4) or alter levels of cytotoxic CD8^{+} T cells among both groups (Figure 4C). Hence the data from our model do not support a role of tumor endothelial IDO1 as a key immunosuppressive feedback mechanism.[46-48] It is tempting to speculate that irradiation does not provide a sufficient proinflammatory cue to induce eIDO to levels relevant to impact T cell infiltration.

While we could confirm the expression of IDO1 in glioma associated ECs and identify distinct endothelial subclusters linked to the CXCL11-CXCR3 axis, our findings did not reveal a significant effect on glioma immunity caused by the loss of eIDO1 in combination with low-dose radiotherapy and adoptive T cell transfer.

## Author Contributions

AAH, KH, MP, and KS conceptualized the studies and designed the experiments. AAH, KH, and TL developed methodologies and performed research and experiments. KJ, CLT, LE, JKS, and AH performed in vitro, in vivo, and ex vivo experiments and in silico analyses. SGM, CAO, CH-M, and FS provided expertise and helped developing methodologies. AAH, MP, and KS wrote the manuscript with input from all co-authors.

## Supplemental Material

Supplemental material for this article is available online.

## REFERENCES

1. Quail DF, Joyce JA. The microenvironmental landscape of brain tumors. *Cancer Cell*. 2017;31:326-341.
2. Ratnam NM, Gilbert MR, Giles AJ. Immunotherapy in CNS cancers: the role of immune cell trafficking. *Neuro Oncol*. 2019;21:37-46.
3. Ochs K, Sahm F, Opitz CA, et al. Immature mesenchymal stem cell-like pericytes as mediators of immunosuppression in human malignant glioma. *J Neuroimmunol*. 2013;265:106-116.
4. Platten M, Nollen EAA, Röhrig UF, Fallarino F, Opitz CA. Tryptophan metabolism as a common therapeutic target in cancer, neurodegeneration and beyond. *Nat Rev Drug Discov*. 2019;18:379-401.
5. Opitz CA, Litzenburger UM, Sahm F, et al. An endogenous tumour-promoting ligand of the human aryl hydrocarbon receptor. *Nature*. 2011;478:197-203.
6. Zhai L, Ladomersky E, Lenzen A, et al. IDO1 in cancer: a gemini of immune checkpoints. *Cell Mol Immunol*. 2018;15:447-457.
7. Chung DJ, Rossi M, Romano E, et al. Indoleamine 2,3-dioxygenase-expressing mature human monocyte-derived dendritic cells expand potent autologous regulatory T cells. *Blood*. 2009;114:555-563.
8. Munn DH, Shafizadeh E, Attwood JT, Bondarev I, Pashine A, Mellor AL. Inhibition of T cell proliferation by macrophage tryptophan catabolism. *J Exp Med*. 1999;189:1363-1372.
9. Hwu P, Du MX, Lapointe R, Do M, Taylor MW, Young HA. Indoleamine 2,3-Dioxygenase production by human dendritic cells results in the inhibition of T cell proliferation. *J Immunol*. 2000;164:3596-3599.
10. Mondal A, Smith C, DuHadaway JB, et al. IDO1 is an integral mediator of inflammatory neovascularization. *EBioMedicine*. 2016;14:74-82.
11. Smith C, Chang MY, Parker KH, et al. IDO is a nodal pathogenic driver of lung cancer and metastasis development. *Cancer Discov*. 2012;2:722-735.
12. Mitsuka K, Kawataki T, Satoh E, Asahara T, Horikoshi T, Kinouchi H. Expression of indoleamine 2,3-dioxygenase and correlation with pathological malignancy in gliomas. *Neurosurg*. 2013;72:1031-1038; discussion 1038-1039.

13. Wainwright DA, Balyasnikova IV, Chang AL, et al. IDO expression in brain tumors increases the recruitment of regulatory T cells and negatively impacts survival. *Clin Cancer Res*. 2012;18:6110-6121.

14. Zhai L, Ladomersky E, Lauing KL, et al. Infiltrating T cells increase IDO1 expression in glioblastoma and contribute to decreased patient survival. *Clin Cancer Res*. 2017;23:6650-6660.

15. Herrera-Rios D, Mughal SS, Teuber-Hanselmann S, et al. Macrophages/microglia represent the major source of indolamine 2,3-dioxygenase expression in melanoma metastases of the brain. *Front Immunol*. 2020;11:120-215.

16. Herrera FG, Ronet C, Ochoa de Olza M, et al. Low-dose radiotherapy reverses tumor immune desertification and resistance to immunotherapy. *Cancer Discov*. 2022;12:108-133.

17. Ochs K, Ott M, Rauschenbach KJ, et al. Tryptophan-2,3-dioxygenase is regulated by prostaglandin E2 in malignant glioma via a positive signaling loop involving prostaglandin e receptor-4. *J Neurochem*. 2016;136:1142-1154.

18. Moon JJ, Chu HH, Hataye J, et al. Tracking epitope-specific T cells. *Nat Protoc*. 2009;4:565-581.

19. Darmanis S, Sloan SA, Croote D, et al. Single-cell RNA-Seq analysis of infiltrating neoplastic cells at the migrating front of human glioblastoma. *Cell Rep*. 2017;21:1399-1410.

20. Mahlokozera T, Patel B, Chen H, et al. Competitive binding of E3 ligases TRIM26 and WWP2 controls SOX2 in glioblastoma. *Nat Commun*. 2021;12:6321.

21. Müller S, Di Lullo E, Bhaduri A, et al. A single-cell atlas of human glioblastoma reveals a single axis of phenotype in tumor-propagating cells. *bioRxiv*. 2018;377606.

22. Speir ML, Bhaduri A, Markov NS, et al. UCSC cell browser: visualize your single-cell data. *Bioinformatics*. 2021;37:4578-4580.

23. Santos JC, Boucher D, Schneider LK, et al. Human GBP1 binds LPS to initiate assembly of a caspase-4 activating platform on cytosolic bacteria. *Nat Commun*. 2020;11:3276.

24. Perng YC, Lenschow DJ. ISG15 in antiviral immunity and beyond. *Nat Rev Microbiol*. 2018;16:423-439.

25. Wang X, Zhang J, Zhou G. The CXCL11-CXCR3A axis influences the infiltration of CD274 and IDO1 in oral squamous cell carcinoma. *J Oral Pathol Med*. 2021;50:362-370.

26. Lo BK, Jalili RB, Zloty D, et al. CXCR3 ligands promote expression of functional indoleamine 2,3-dioxygenase in basal cell carcinoma keratinocytes. *Br J Dermatol*. 2011;165:1030-1036.

27. Alva JA, Zovein AC, Monvoisin A, et al. VE-cadherin-cre-recombinase transgenic mouse: a tool for lineage analysis and gene deletion in endothelial cells. *Dev Dyn*. 2006;235:759-767.

28. Kesarwani P, Prabhu A, Kant S, et al. Tryptophan metabolism contributes to radiation-induced immune checkpoint reactivation in glioblastoma. *Clin Cancer Res*. 2018;24:3632-3643.

29. Prins RM, Odesa SK, Liau LM. Immunotherapeutic targeting of shared melanoma-associated antigens in a murine glioma model. *Cancer Res*. 2003;63:8487-8491.

30. Besser MJ, Schallmach E, Oved K, et al. Modifying interleukin-2 concentrations during culture improves function of T cells for adoptive immunotherapy. *Cytotherapy*. 2009;11:206-217.

31. Hanada KI, Yu Z, Chappell GR, Park AS, Restifo NP. An effective mouse model for adoptive cancer immunotherapy targeting neoantigens. *JCI Insight*. 2019;4:e124405.

32. Platten M, Friedrich M, Wainwright DA, Panitz V, Opitz CA. Tryptophan metabolism in brain tumors - IDO and beyond. *Curr Opin Immunol*. 2021;70:57-66.

33. Günther J, Däbritz J, Wirthgen E. Limitations and off-target effects of tryptophan-related IDO inhibitors in cancer treatment. *Front Immunol*. 2019;10:1801.

34. Labadie BW, Bao R, Luke JJ. Reimagining IDO pathway inhibition in cancer immunotherapy via downstream focus on the tryptophan-kynurenine-aryl hydrocarbon axis. *Clin Cancer Res*. 2019;25:1462-1471.

35. Zhai L, Ladomersky E, Dostal CR, et al. Non-tumor cell IDO1 predominantly contributes to enzyme activity and response to CTLA-4/PD-L1 inhibition in mouse glioblastoma. *Brain Behav Immun*. 2017;62:24-29.

36. Komotar RJ, Otten ML, Moise G, Connolly ES Jr. Radiotherapy plus concomitant and adjuvant temozolomide for glioblastoma-a critical review. *Clin Med Oncol*. 2008;2:421-422.

37. Tokunaga R, Zhang W, Naseem M, et al. CXCL9, CXCL10, CXCL11/CXCR3 axis for immune activation - a target for novel cancer therapy. *Cancer Treat Rev*. 2018;63:40-47.

38. Cole KE, Strick CA, Paradis TJ, et al. Interferon-inducible T cell alpha chemoattractant (I-TAC): a novel non-ELR CXC chemokine with potent activity on activated T cells through selective high affinity binding to cxcr3. *J Exp Med*. 1998;187:2009-2021.

39. Walters MJ, Ebsworth K, Berahovich RD, et al. Inhibition of CXCR7 extends survival following irradiation of brain tumours in mice and rats. *Br J Cancer*. 2014;110:1179-1188.

40. Würth R, Barbieri F, Bajetto A, et al. Expression of CXCR7 chemokine receptor in human meningioma cells and in intratumoral microvasculature. *J Neuroimmunol*. 2011;234:115-123.

41. Calatozzolo C, Canazza A, Pollo B, et al. Expression of the new CXCL12 receptor, CXCR7, in gliomas. *Cancer Biol Ther*. 2011;11:242-253.

42. Sonar SA, Shaikh S, Joshi N, Atre AN, Lal G. IFN-γ promotes transendothelial migration of CD4(+) T cells across the blood-brain barrier. *Immunol Cell Biol*. 2017;95:843-853.

43. Dangaj D, Bruand M, Grimm AJ, et al. Cooperation between constitutive and inducible chemokines enables T cell engraftment and immune attack in solid tumors. *Cancer Cell*. 2019;35:885-900.e10.

44. Lai JZ, Zhu YY, Ruan M, Chen L, Zhang QY. Local irradiation sensitized tumors to adoptive T cell therapy via enhancing the cross-priming, homing, and cytotoxicity of antigen-specific CD8 T cells. *Front Immunol*. 2019;10:2857-2914.

45. Weiss T, Weller M, Guckenberger M, Sentman CL, Roth P. NKG2D-based CAR T cells and radiotherapy exert synergistic efficacy in glioblastoma. *Cancer Res*. 2018;78:1031-1043.

46. Georganaki M, Ramachandran M, Tuit S, et al. Tumor endothelial cell up-regulation of IDO1 is an immunosuppressive feed-back mechanism that reduces the response to CD40-stimulating immunotherapy. *OncoImmunology*. 2020;9:1730538.

47. Kocher F, Amann A, Zimmer K, et al. High indoleamine-2,3-dioxygenase 1 (IDO) activity is linked to primary resistance to immunotherapy in non-small cell lung cancer (NSCLC). *Transl Lung Cancer Res*. 2021;10:304-313.

48. Li H, Bullock K, Gurjao C, et al. Metabolomic adaptations and correlates of survival to immune checkpoint blockade. *Nat Commun*. 2019;10:4346-4348.